Microbial communities from Arctic marine sediments respond slowly to methane addition during *ex situ* incubations

Scott Klasek[1], Marta E. Torres[2], Douglas H. Bartlett[3], Madeline Tyler[1], Wei-Li Hong[4**], Frederick Colwell[1,2*]

1 Department of Microbiology, Oregon State University, Corvallis, OR, USA

2 College of Earth, Ocean, and Atmospheric Sciences, Oregon State University, Corvallis, OR, USA

3 Marine Biology Research Division, Scripps Institution of Oceanography, University of California, San Diego, CA, 92093-0202, USA

4 Centre for Arctic Gas Hydrate, Environment and Climate (CAGE), Department of Geosciences, UiT The Arctic University of Norway, N-9037 Tromsø, Norway

* Address correspondence to Frederick Colwell, rcolwell@coas.oregonstate.edu.

** Present address: Wei-Li Hong, Geological Survey of Norway, NO-7491 Trondheim, Norway

Keywords: methane, AOM, sulfate reduction, marine sediments, Arctic, microbial communities, pressure incubation

Running title: Community changes in incubated Arctic marine sediments

Funding sources: DOE, Deep Carbon Observatory

Summary

Anaerobic methanotrophic archaea consume methane in marine sediments, limiting its release to the water column. However, their responses to changes in methane and sulfate remain poorly constrained. To address how methane exposure may affect microbial communities and methane- and sulfur-cycling gene abundances in Arctic marine sediments, we collected sediments from offshore Svalbard that represent three geochemical horizons where anaerobic methanotrophy is expected to be active, previously active, and long-inactive. Sediment slurries were incubated at *in situ* temperature and pressure with different added methane concentrations, and then studied for extended incubation times. Rapid increases in sulfur-cycling Deltaproteobacteria occurred after 30 days in previously active and long-inactive sediments. However, these sediments showed no evidence of methanotrophy after nearly eight months of incubation. Sediments from an active area of seepage began to reduce sulfate in a methane-dependent manner within months, preceding increased relative abundances of anaerobic methanotrophs ANME-1 within communities. However, methane did not structure microbial community changes across any incubation time or sediment type. These results suggest that active anaerobic methanotrophic populations may require years to develop, and that microbial community composition may affect methanotrophic responses to potential large-scale seafloor methane releases in ways that may provide insight for future modeling studies.

Originality-significance statement

Microbial communities that consist of anaerobic methanotrophic archaea, sulfate-reducing bacteria, and many others remove most of the methane produced in marine sediments worldwide, but are thought to develop over timescales of years and are challenging to study *in situ*. In this novel study, we describe concomitant observations of microbial community composition, methanotrophic activity, and abundances of methane- and sulfur-cycling genes to characterize responses of distinct sediment zones to varying methane concentrations across timescales of months. Our finding that microbial community changes precede growth and activity of methanotrophic populations illuminates the role of microbial community dynamics on methane flux to the overlying hydrosphere.

Introduction

Globally, marine sediments are sources and sinks of tens to hundreds of teragrams of methane per year (Valentine, 2002). Gas hydrates, vast reservoirs of temperature-sensitive methane, can be found in Arctic sediments below only hundreds of meters of water depth, and thus are expected to be influenced more quickly by warming than hydrates at lower latitudes (Hunter *et al.*, 2013). Offshore western Svalbard, models of hydrate stability based on ocean warming trends predict increases in seafloor methane flux from slope and shelf regions (James *et al.*, 2016 and references therein). Seafloor methane leakage along Arctic continental margins (Shakhova *et al.*, 2010; Mau *et al.*, 2017), has triggered concerns that warming bottom waters will destabilize hydrates, increasing methane influx into the water column or even the atmosphere (Westbrook *et al.*, 2009). Though there is no evidence that this is presently occurring (Berndt *et al.*, 2014; Hong *et al.*, 2017; Wallmann *et al.*, 2018), methane production,

consumption, and transport in Arctic seabed environments is complex and spatiotemporally variable.

Anaerobic methane oxidation (AOM) is a crucial biofilter that prevents up to 90% of this methane from reaching the hydrosphere (Reeburgh, 2007; Boetius and Wenzhöfer, 2013). This process, mediated by several clades of anaerobic methanotrophic archaea (ANME) and distributed in marine sediments worldwide, uses sulfate as an electron acceptor:

$CH_4 + SO_4^{2-} \rightarrow HCO_3^- + HS^- + H_2O$ (Equation 1)

To accomplish AOM, ANME often associate with sulfate-reducing bacteria (SRB) at sulfate-methane transition zones (SMTs), sediment horizons where sulfate reduction (SR) and AOM remove sulfate and methane from porewaters (Knittel and Boetius, 2009). Their global ubiquity and distribution within methane-rich sediments (Nunoura *et al.*, 2008; Ruff *et al.*, 2015) shapes microbial community structures in these zones (Harrison *et al.*, 2009), and *in situ* observations suggest that these methanotrophic communities develop on timescales of years (Ruff *et al.*, 2018; Klasek *et al.*, 2019). Processes that could alter the distribution of methane and sulfate throughout the sediment column, such as changes in subseafloor methane flux (Hong *et al.*, 2016), emission of mud breccia flows through mud volcanism (Ruff *et al.*, 2018; Klasek *et al.*, 2019), and sediment gravity flows (Hensen *et al.*, 2003), all presumably impact microbial community structure, ANME/SRB populations, and ultimately AOM rates.

How ANME and other sediment microbial community members respond to changes in methane fluxes remains unclear, and represents a critical knowledge gap for understanding how a large-scale seafloor methane release could be mitigated in high-latitude regions (Dale *et al.*, 2008). Though ANME have not been isolated in pure culture (Wegener *et al.*, 2016), enrichment studies have characterized their doubling times on the order of months (Nauhaus *et al.*, 2007). Incubations at elevated pressure, which increases methane solubility in the aqueous phase, have successfully stimulated AOM in a methane-dependent manner (Nauhaus *et al.*, 2002; Deusner *et al.*, 2010), enriched microbial biomass (Girguis *et al.*, 2005; Wang *et al.*, 2014), and characterized differences in temperature and pressure optima between ANME subpopulations (Nauhaus *et al.*, 2005; Timmers *et al.*, 2015; Bhattarai, Zhang, *et al.*, 2018).

Our objective was to determine how microbial communities and ANME and SRB numbers would respond to changing methane fluxes in Arctic marine sediments in a controlled incubation. We collected marine sediments from seafloor gas hydrate mounds (GHMs) at Storfjordrenna, offshore Svalbard (Fig. 1) that emit methane into the overlying water and lie at depths corresponding to upper limits of gas hydrate stability (Serov *et al.*, 2017). Three sediments with varying inferred AOM activity (Hong *et al.*, 2017) were amended with methane and incubated at *in situ* temperature and pressure for up to eight months. We anticipated that 1) highest community changes would be observed in *PA* and *IA* sediments as microbial communities adjusted to geochemical perturbations; 2) SR-AOM rates would depend on added methane concentrations and take longer to establish in *PA* and *IA* sediments; and 3) correlations would be seen between SR-AOM rates and ANME/SRB marker gene abundances.

Results

To investigate how methane concentrations structure different microbial communities and control SR-AOM rates, we conducted several long-term (several month) microcosm incubations of Arctic marine sediments that varied with respect to their predicted AOM capability. We first consider *in situ* geochemical distinctions between each of the sediment types, and then discuss geochemical changes observed during incubations. These provide context for subsequent assessment of microbial community and gene abundance changes during incubation.

Incubated sediments were selected to reflect predicted patterns of spatiotemporal variability in AOM activity across the Storfjordrenna GHM area, based on rate data derived from transport-reaction models inferred from shapes of porewater sulfate profiles (Borowski *et al.*, 1996; Dale *et al.*, 2008). At Storfjordrenna, increases in subsurface methane flux that coincide with seepage atop several GHMs have been attributed to venting of deep reservoirs (Hong *et al.*, 2017). A push core sample from an active site of seepage (PC1029 at 30-40 cm, from GHM3) was collected from just below a sediment depth where remaining porewater sulfate indicated incomplete reduction and directly atop gas hydrate nodules recovered at 45 cmbsf (Fig. 1B). Methane phase transitions and an abrupt decrease in porewater sulfate with depth throughout this core suggest this horizon was undergoing AOM at the time of sampling, and we designate this sample as active ("*A*") for future reference. At the southern flank of GHM3, a sample from 80-90 cm at GC1045 lies just below a sulfate-methane transition where alkalinity has increased through the sulfate reduction zone in an equimolar fashion (Fig. 1C). The curvature of the sulfate profile is consistent with a recent increase in methane flux at this site. A modeling study of a core from the same area (Hong *et al.*, 2017) detailed an increase in methane flux pushing the SMT upwards at a rate of approximately 10 cm per year. This suggests the GC1045 80-90 cm sample may have been mediating AOM only a few years before sampling, and we designate this sample as previously active ("*PA*"). At GC1036, away from the GHMs, sulfide was not detected and porewater alkalinity was elevated only slightly above seawater values (Fig. 1D). The gradual decrease in porewater sulfate concentrations points towards a low level of methane flux at this location. The redox chemistry at 20-35 cm appears to be uninfluenced by any recent methane incursion, suggesting this zone has not recently undergone AOM. We refer to this sample as inactive ("*IA*").

When *A* sediments were incubated at *in situ* pressure (experimental setup shown in Fig. S1), a methane-dependent increase in media sulfide and a concomitant decrease in sulfate were observed after 118 days, with even stronger changes shown in the later stages of the 222-day incubation (Figs. S2 & S3). Incubations amended with methane showed similar increases in media DIC (Fig. S4). These observations indicate that porewater chemistry changes due to stimulation of AOM occurred sometime between two and four months after incubations began. Methane-free controls allow us to quantify baseline sulfate reduction rates attributed to organic matter oxidation, as others have done (Nauhaus *et al.*, 2005; Deusner *et al.*, 2010; Zhang *et al.*, 2010). Although some SR was coupled to oxidative breakdown of organic matter, it never exceeded 62% of the rate measured in corresponding incubations with 5 mM CH_4 (*A* sediments from 0-101 days, Fig. 2). These data indicate that a significant fraction of the sulfate is consumed by AOM. SR rates for intervals of 118- and 222-day incubations increased with time and added methane, and exceeded rates measured in other sediment incubations (Fig. 2).

Stoichiometrically, sulfate consumed an average of 98% of the added methane in the *A* incubations, far more than in the other sediments, but the $SO_4^{2-}{}_{consumed}/CH_{4\ added}$ ratio ranged from zero (in incubation stages where sulfate did not decrease) to 2.3 during the 30-101 days incubation interval of sample *A* amended with 1.5 mM CH_4. SR rates exceeded sulfide production rates in incubations with added methane, indicating precipitation of sulfide minerals. During AOM-SR, the $\delta^{13}C$–DIC pool becomes more depleted due to preferential selection of ^{12}C-CH_4 by methanotrophs (Borowski *et al.*, 1997), with a characteristic kinetic isotope fractionation effect (ε). We estimated a value for ε, and show that during our incubations of *A* samples it decreases from 42‰ to 19‰ in a methane-dependent manner (Fig. 3). Values of ε below 30 are generally indicative of AOM (Whiticar, 1999).

In contrast to the *A* incubations, the *IA* and *PA* sediment microcosms showed little to no sulfide buildup or sulfate consumption (Figs. S2 & S3, Table 1) and and there is no evidence of methane-dependent SR at any point during the timeseries (Fig. 2). Values of ε did not reliably decrease when amended with 5 mM methane (Fig. 3, Table 1). Collectively these data show that AOM was not detected, even after nearly eight months, in *IA* and *PA* incubations.

Microbial communities from the three sediment types differed before incubations began (Table S1A). The *A* sediment communities consisted of mainly Epsilonproteobacteria and ANME (within class Methanomicrobia), while the *IA* was dominated by Deltaproteobacteria and the *PA* by Atribacteria (Fig. 4). *PA* sediments, sampled from below a sulfate reduction zone, were comparatively lower in OTU richness than *IA* (Fig. S5), in line with patterns of community diversity and assembly documented across SMTs (Starnawski *et al.*, 2017). ANMEs constituted 5% of the *PA* sediment community, and were not detected in the *IA* sediment. Nevertheless, many overlapping classes were common to all three communities. Highest richness was seen in the *IA* sediment community (Fig. S5). During sample storage at 4˚C after collection, *IA* and *PA* sediment communities showed reduced alpha diversity and increases in percent abundances of *Deltaproteobacteria,* but the *A* community did not change appreciably over nearly a year (Fig. S5).

Surprisingly, addition of methane did not broadly alter community structure in any sediment type (all $p>0.6$, Table S1B). Methane addition significantly ($\alpha=0.05$) increased percent abundances of only three OTUs that comprised over 1% of their communities. These included *Draconibacterium* and *Desulforhopalus* in *A* sediment communities, and a *Desulfuromonas* in the *PA* that was most similar to *D. svalbardensis*, a psychrophile that couples acetate oxidation to Fe (III) reduction (Vandieken, 2006).

Sediment microbial communities, particularly the *IA* and *PA*, shifted noticeably after only 30 days of incubation, regardless of added methane concentration (Fig. 5). These changes first included increased percent abundances of Deltaproteobacteria, while eventually Clostridia and Bacteroidia became more dominant in longer incubations (Fig. 4). Longer incubations saw continued community changes in all but one instance (*PA* sediments between 118 and 222 days, Fig. 5). In contrast to the patterns of SR-AOM observed during incubation, the *IA* sediment communities changed the most over time, and the *A* communities the least (Table 1). Though *IA*

and *PA* communities incubated for 222 days appear on the right side of the NMDS plot (Fig. 5), they still show discrete clustering by sediment type. Thus, across all incubations, we observe little evidence of convergence towards a common community structure.

Across all sediment types, percent abundances of twenty highly abundant OTUs changed when incubated for different times (Fig. 6). Many of these dynamic OTUs belong to the class *Deltaproteobacteria* and are implicated in sulfur cycling in anoxic marine sediments. Some (unclassified *Desulfuromonadales*) increased or decreased depending on the sediment type, while in other instances, different OTUs within the same genus (*Desulfocapsa* OTUs 4 and 5) show different concurrent responses within the same community. ANME percent abundances showed time-dependent changes, with ANME-1b increasing in the *A* sediment communities between 30 and 118 days, and ANME-2a-2b decreasing in the *PA* communities from 118 to 222 days. Percent abundances of some taxa, particularly *Deltaproteobacteria*, increased as samples were stored at 4˚C and atmospheric pressure prior to incubation (Fig. S5), and these largely concurred with the community shifts seen in the first month of incubations (Fig. 4). Two genera from the *PA* communities, *Desulfuromonas* and *Lutibacter*, increased significantly during storage. This made it appear that they had decreased over the final several months of incubations, so OTUs belonging to these groups were removed from Fig. 6.

The genes *mcrA* and *dsrAB* were quantified to represent abundances of anaerobic methanotrophs (Luton *et al.*, 2002; Hallam *et al.*, 2003) and dissimilatory sulfate reducers (Leloup *et al.*, 2004), respectively. Before incubation, *mcrA* concentrations across the three sediment types differed by several orders of magnitude, with the *IA* sediments showing the lowest, and the *A* sediments showing the highest levels of this functional gene (Fig. 7A). Differences in *dsrAB* genes were less notable, but lowest concentrations were seen in the *PA* sediments (Fig. S6A). Together, these patterns in gene abundances are consistent with the commonly understood spatial/redox distribution of methane- and sulfur-cycling microbes through the sediment column.

During incubation, *mcrA* gene abundances only increased with incubation time and methane concentration in *PA* sediments. Because ANME did not increase among *PA* incubations, this could be attributed to slight increases in canonical methanogenic taxa (non-ANME *Methanomicrobia*) from 0.05 to 0.2% of *PA* communities over the incubation period ($p=0.0254$, one-way ANOVA). *Methanococcoides* was the most abundant methanogenic genus throughout *PA* communities (0.06% on average), but neither it nor other genera showed clear time- or methane-dependent changes in percent abundance. *mcrA* concentrations in *IA* sediments did not change over incubation time (Fig. 7A, Table 1) and did not correlate with percent abundances of ANME or canonical methanogens, the latter of which averaged only 0.05% of *IA* communities. Changes in *dsrAB* abundances were more dynamic: *IA* incubations showed time-dependent increases, while the *PA* incubations showed increases over the first 30 days followed by a slight decline at 222 days (Fig. S6A). Though *A* communities did not show significant changes in *mcrA* or *dsrAB* numbers throughout all incubation times and methane concentrations, percent abundances of ANME-1 OTUs increased in a methane-dependent manner after 222 days, while those belonging to ANME-2 showed little change (Fig. 7B). Across

A sediment communities, ANME comprised 13% of sequences, 80 times more abundant than canonical methanogens.

In contrast to *A* incubations, *IA* and *PA* communities showed negligible changes in ANME (<0.1% abundance) when amended with methane. ANME-3 were either of insignificant abundance or not detected across the entire dataset. A positive correlation was observed between SR rates and *mcrA* gene abundances in the *A* samples incubated for 118 or 222 days (Fig. 7C). Interestingly, we found no correlation between SR rates and *dsrAB* gene abundances (Fig. S6B). Rather, the methane concentrations supplied to these incubations appeared to limit SR-AOM rates to a greater extent than the levels of either gene.

Discussion

Anaerobic methanotrophic archaea consume methane produced in marine sediments, limiting its release to the water column, yet their response to changes in methane and sulfate remain poorly constrained. To better understand how methane concentrations influence microbial community structure and activity under *in situ* conditions, we incubated three sediments of varying predicted AOM capability at *in situ* pressure and with amended methane concentrations on months-long timescales. We open the discussion by considering how changes in methane supply over time influence incubation geochemistry and activity as measured by SR-AOM rates, which provides subsequent context for how these variables alter microbial community dynamics. We finally discuss how this information derived from an *ex situ* laboratory incubation study can be applied to analyze AOM dynamics and microbial communities in seafloor environments.

Incubation geochemistry

As ^{12}C-methane is preferentially oxidized to DIC by microbes in marine sediments, the residual methane pool becomes isotopically heavier, resulting in a kinetic isotope effect (ε) ranging from 4-30‰. In contrast, acetoclastic methanogenesis produces ε values ranging from 35 to 55‰ (Whiticar, 1999). The *A* incubations that showed high SR rates and a decrease in ^{13}C in the DIC pool suggest anaerobic methane oxidation, with ε values ranging from around 37‰ to as low as 19‰ in the late-term incubations amended with 5 mM methane (Fig. 3). These depletions occurred despite resupplying each incubation interval with methane from a tank, which had a CH_4 composition of -35‰. In the *PA* incubations, the decrease in ε seen after 60 days may signal a slight shift towards AOM, but without any observation of methane-dependent SR, organoclastic SR may be more likely. Other reports of incubated microbial consortia mediating SR-AOM resulted in depletion of δ^{13}C-CH_4, which was attributed to co-occurring methanogenesis (Seifert *et al.*, 2006) and/or carbon isotope equilibration during sulfate limitation (Yoshinaga *et al.*, 2014). However, because we did not observe depletion of sulfate (below 1 mM) or relative increases in methanotrophic taxa, these two processes likely did not occur in our incubations.

Because methane solubility in seawater increases with pressure, prior incubations of methane-rich seafloor sediments have shown that AOM rates increase with methane partial pressures over a broad timescale, ranging from days to months (Nauhaus *et al.*, 2002; Meulepas *et al.*, 2009; Deusner *et al.*, 2010; Zhang *et al.*, 2010). In most of these studies, no lag times were

observed before AOM was stimulated, though Meulepas et al. (2010) suggested that sulfate reduction coupled to organic matter breakdown may delay the onset of AOM during enrichment (Meulepas *et al.*, 2009). We see a similar lag in initial stages of 222-day incubations of *A* sediments, where sulfate reduction rates are comparable among all methane treatments, but in later stages of *A* incubations, sulfate reduction rates were higher with added methane (Fig. 2).

In contrast to what we observed in our *PA* sediment incubations, AOM has been stimulated in previously oxic, non-seep sediments amended with methane after 24 weeks of continuous-flow incubation (Girguis *et al.*, 2003). Overall, enrichment studies have yielded maximum SR-AOM rates that vary several orders of magnitude, from 0.1 to 286 μmol g dry weight^{-1} day^{-1} (Meulepas *et al.*, 2009). Assuming a sediment porosity of 0.5 and a density of 2.6 g/ml, our *A* incubation maximum measured rate of 0.91 μmol g dry weight^{-1} day^{-1} appears on the low end of this range, but is comparable to other long-term incubations where ANME were enriched (Bhattarai *et al.*, 2018). SR-AOM rates from our incubations are comparable to, or even an order of magnitude higher than, the numerically-derived rates from Vestnesa Ridge, west of Svalbard (Hong *et al.*, 2016) despite the fact that methane concentrations in our incubations remained far below saturation. This may reflect different flow regimes at these sites, particularly between the *A* samples collected from an active seep and the Vestnesa SMTs that have lower fluxes of sulfate and methane. Other discrepancies in incubation rate measurements may be attributed to different methods used in sediment storage and rate calculation (Krüger *et al.*, 2008), variations in methane and/or sulfate supply between batch and flow-through incubations (Zhang *et al.*, 2010), physical parameters including pressure and temperature (Nauhaus *et al.*, 2002), and variability in microbial community composition.

Methane-associated microbial community changes

We observed a limited effect of methane on microbial community structure across timescales of months in incubations that simulated seafloor conditions. Total percent abundances of ANME-affiliated reads increased from 8% to 15-20% in the *A* communities amended with either 1.5 or 5 mM methane, but differences were not apparent until 222 days (Fig. 7B, Table S3). After several months of high-pressure incubations targeting AOM, similar studies reported increases in ANME 16S genes (Girguis *et al.*, 2005), cells and aggregates (Zhang *et al.*, 2014), and percent abundances in archaeal communities from <1% to up to 50-60% (Aoki *et al.*, 2014; Bhattarai *et al.*, 2018). Years of enrichment with methane and sulfate were required for ANME and SRB to attain near-dominance of archaeal and bacterial communities (Wegener *et al.*, 2016). Earlier studies that enriched ANME noted doubling times varying from 1.1 to 7.5 months (James *et al.*, 2016, and references therein). The *A* incubations that exhibited highest SR-AOM rates showed increases in *mcrA*; assuming one copy of *mcrA* per ANME genome (Haroon *et al.*, 2013), these increases translate to doubling times of 7.6 months which are similar to previously observed doubling times of up to seven months (Nauhaus *et al.*, 2007). Known methanogens, including recently established methane-cycling clades such as Bathyarchaeota (Evans *et al.*, 2015) and Verstraetearchaeota (Vanwonterghem *et al.*, 2016), were nearly two orders of magnitude less abundant than ANME in *A* communities, supporting the validity of this calculation. In contrast to (Zhang *et al.*, 2014), who saw bacterial alpha diversity increase after incubations, we observed no such diversity changes associated with incubation (data not

shown) and even saw a decrease in alpha diversity associated with storage time in A_t and B_t samples (Fig. S5).

In the *A* sediment communities, *Draconibacterium* and *Desulforhopalus* OTUs proliferated in response to methane addition. *Draconibacterium* is a recently-described genus of facultative anaerobes from marine environments capable of fermenting polysaccharides (Du *et al.*, 2014; Li *et al.*, 2016). Members of *Desulforhopalus* reduce sulfate with lactate, propionate, alcohols, or aminosulfonic acids (Isaksen and Teske, 1996; Lie *et al.*, 1999), and thus their presence may reflect organoclastic sulfate reduction concurrent with SR-AOM.

Temporal community changes

Microbial community structure in all sediment types changed with the length of time they were incubated (Fig. 5) and not with the amount of methane they were amended with (Table S1). Nevertheless, shifts in microbial community structure were highest in samples from above or below SMTZs, which may reflect potential geochemical redox changes associated with incubation: *IA* sediments were introduced to sulfide in seawater media, while *PA* sediments were re-exposed to sulfate. Proliferation of an ANME-1b OTU between 30 and 118 days in T sediments (Fig. 6) coincides with, and may account for, the increase in AOM-SR rate during this interval (Fig. 2). Sulfide never accumulated over 3 mM in media from *IA* or *PA* incubations (Fig. S2), so microbial communities likely did not experience sulfide toxicity, which has been noted to occur around 5 mM or more (Maillacheruvu and Parkin, 1996). Increases in *dsrAB* among *IA* and *PA* 30-day incubations (Fig. S6) probably reflect the proliferation of sulfate-reducing clades of Deltaproteobacteria (Fig. 4), but they apparently mediate different cycles or do not reduce sulfate until later stages of incubation. Alpha- and Gammaproteobacteria, which possess oxidative types of *dsrAB* (Müller *et al.*, 2015), could also partially account for the increase in *dsrAB*. Because no sulfate reduction was observed at 30 days, high abundances of sulfur-cycling taxa may reflect other processes such as sulfide oxidation with organic matter (Heitmann and Blodau, 2006). Though *mcrA* abundances increased most quickly in *PA* incubations amended with highest amounts of methane (Fig. 7A), ANME percent abundances did not change appreciably (Table 1). Instead, this increase could reflect growth of methanogens, which can be active even in methane concentrations of several mM (Lazar *et al.*, 2012). OTUs belonging to the methanogenic clade *Methanococcoides* increased very slightly, from 0.04% to 0.21% after 222 days. *Methanococcoides* also increased up to 0.4% in *IA* communities, where ANMEs were only sporadically detected. Though some of the *mcrA* detected could reflect non-Euryarchaeotal lineages (Evans *et al.*, 2015; Vanwonterghem *et al.*, 2016), these recently-described potential methane-cycling phyla were very sparsely detected (Bathyarchaeota) or nonexistent (Verstraetearchaeota) in our communities.

The *IA* communities saw growth of OTUs belonging to *Geopsychrobacter* and *Desulfuromonas* (Fig. 6). These genera are capable of using acetate and a variety of other organic compounds derived from fermenters as electron donors, and Fe (III), Mn (IV), or S_0 as electron acceptors (Pfennig and Biebl, 1976; Roden and Lovley, 1993; Holmes *et al.*, 2004). Since Fe (II) concentration peaked at over 19 µM within the *IA* sediment depth, this Fe (II) produced

through iron reduction could precipitate sulfide as iron sulfide minerals and account for the lack of sulfide accumulation observed in corresponding incubations (Fig. S2).

The *A* communities changed over time, but to a lesser degree than reported in a five-year enrichment with methane at ambient pressure (Aoki *et al.*, 2014). No changes in *mcrA* or *dsrAB* abundance were observed in these incubations. This suggests that communities were already acclimated for AOM, and also that approximately eight months of incubation did not stimulate much ANME/SRB growth at the methane concentrations and conditions provided. However, a positive relationship between SR-AOM rate and *mcrA* abundance appears dependent on methane addition (Fig. 7C). In two outliers, *mcrA* exceeded 10^8 copies g^{-1}, suggesting growth of ANME or other methanotrophic taxa that contain this gene. However, in the other incubations AOM-SR instead appeared to be driven by an increase in ANME activity.

Community activity *in situ*

Several factors need to be considered when interpreting incubation studies to infer *in situ* microbial community function and dynamics. Dilutions and "bottle effects" (Hammes *et al.*, 2010) can alter bacterial community activity (Stewart *et al.*, 2012) possibly due to organic matter flocculation (Pernthaler and Amann, 2005). We observed an unexpected proliferation of Bacteroidia and Clostridia in our incubations, considering each class comprised around 0.01% of sequences from cores collected *in situ* at the same GHM area (data not shown). *Methanococcoides*, *Geopsychrobacter* and *Draconibacterium* were also barely detected *in situ*, which suggests that conditions pertaining to incubation, potentially related to organic carbon turnover, may influence community composition. Though we replaced media periodically to limit sulfide accumulation, continuous-flow high pressure enrichment strategies would further minimize buildup of toxic metabolites (Zhang *et al.*, 2010). These approaches, combined with high-pressure sediment coring, better approximate *in situ* physical and geochemical conditions while allowing experimental manipulation (Case *et al.*, 2017).

Our finding that microbial communities, when supplied with methane and sulfate, may change significantly over several months without any apparent AOM activity suggests that incubations aiming to understand details of AOM adaptation under different conditions would likely require timescales of years. Field studies combining community analysis with seafloor observatory data across recent eruptions at a seafloor mud volcano found that AOM communities develop on timescales of 2-5 years (Ruff *et al.*, 2018). Across a permafrost thaw gradient associated with decade-scale changes in vegetation, shifts in methanogenic communities and the dominance of acetoclastic methanogenesis have been associated with increased atmospheric methane fluxes (McCalley *et al.*, 2014). In contrast, active communities of aerobic methanotrophic bacteria in wetland soils are capable of changing composition within a week after exposure to higher methane concentrations (Knief *et al.*, 2006). In our incubations, increased percent abundances of several clades of sulfate-reducing bacteria appear to represent a stage that precedes AOM establishment that is consistent with field observations. The lack of activity in *PA* sediments is surprising, considering that ANME are present and the sediment likely corresponded with a SMT only years before sampling (Hong *et al.*, 2017). In contrast, sediments from an active seep showed increases in SR-AOM rates that corresponded with higher abundances of *mcrA* genes and percent abundances of ANME. Microbial community data may be of use when paired with

geochemical markers to further elucidate methane seepage in areas with spatiotemporally heterogeneous methane fluxes (Hong *et al.*, 2018).

Model-based approaches concerning changes in the activity or efficiency of the subseafloor microbial methane filter, possibly from increasing subseafloor methane fluxes (Dale *et al.*, 2008; Boetius and Wenzhöfer, 2013), should consider realistic timescales for microbial community responses within particular sediment horizons. Our interpretations that zones previously capable of AOM may remain dormant after months of incubation with methane and sulfate suggest longer-term characterization of these lag times is needed to fully understand the development of methanotrophic communities in sediments. We further posit that *ex situ* incubations allow cross-validation of complementary field studies on AOM development, and aid in determining causative relationships between microbial community structure and biogeochemical function.

Fundamentally, it can be quite challenging to conduct controlled long-term experiments in the field, and these experiments may also be subject to some bias. By using laboratory experimentation to study microbial communities under defined conditions, such as increases in temperature (Fuchs *et al.*, 2016) or organic matter concentrations (Babbin *et al.*, 2016), novel insight can be gained into causal relationships among biogeochemical processes that exist in nature, and how these processes might be expected to change in response to environmental stimuli. Ideally, both controlled laboratory incubations and careful experiments performed at field sites can function together as complementary approaches to resolve difficult microbial ecology issues.

Experimental Procedures

Fieldwork and sample collection

Sediment samples were collected aboard the RV Helmer Hanssen on cruise CAGE16-5, from June 16th to July 4th, 2016, at the mouth of the Storfjordrenna trough fan, offshore Svalbard (Fig. 1A) with gravity cores or push cores. Gravity core (GC) 1045 was recovered from the south slope of GHM3, while GC1036 was collected several km east of GHM3 in 394 m water depth. Once cores were recovered, their plastic liners were removed from the core barrel, sectioned into 1 m segments, labeled, and split in half with a table saw to obtain working and archive halves. Core halves were stored horizontally at 4˚C for up to two hours while alkalinity measurements were taken. Replicate PVC push cores (PC1029) for geochemical and microbiological sampling were collected approximately 30 cm from observed bubble seepage at GHM3 using a Sperre Subfighter 30k remotely operated vehicle (ROV) from the Centre for Autonomous Marine Operations and Systems (AMOS) equipped with a video camera and a raptor arm. Cores were extruded and subsampled using PVC tubing.

Sample selection for microbiology targeted discrete sediment horizons where AOM was predicted to be inactive (*IA*), previously active (*PA*), and active (*A*). These designations were inferred through porewater sulfate profiles (Fig. 1B-D), wherein nonlinear decreases in sulfate with depth have been attributed to the encroachment of AOM into shallow sediment horizons as a result of increased subsurface flux (Hong *et al.*, 2017). These three samples corresponded roughly to geochemical zones located above, below, and within SMTs, whose depths were

inferred by onboard porewater alkalinity titrations from the three cores and later bolstered by porewater sulfate profiles (Fig. 1B-D). The low-alkalinity inactive (*IA*) sample was collected from GC1036 at 20-35 cm below seafloor, and the previously active (*PA*) sample was taken from GC1045 at 80-90 cm depth, just below the porewater alkalinity increase corresponding to the SMT. The active (*A*) sample, at 30-40 cm from PC1029, was chosen because it lay below an alkalinity increase but above gas hydrates recovered at 45 cm (Fig. 1B).

Using ethanol-sanitized spatulas to scrape away the outer few mm of sediment from the working core half, sediment samples were placed into Gaspak anaerobic pouches with oxygen-scavenging catalysts (BD Biosciences) and stored in a nitrogen-filled bag at 4˚C until the cruise ended, then transported to Oregon State University on ice. Unincubated subsamples were frozen immediately after collection. Samples were stored in anaerobic pouches in a cold room for 100 to 242 days until incubations began. Anaerobic methanotrophic communities are thought to be resilient to pressure changes of these magnitudes (0.1 to 4 MPa); pressures up to 20 MPa have been required to significantly alter composition of enriched methanotrophic communities (Bhattarai, Zhang, *et al.*, 2018).

Incubation

A manual pressure pump generator (High Pressure Equipment Co. part 87-6-5) was used to hydrostatically pressurize standard or customized pressure vessels to 4.0 MPa, approximating *in situ* pressure (Fig. S1A). At this pressure, and at an incubation medium salinity of 35 ppt, hydrate can form between 3.0 and 3.1˚C, provided sufficient methane concentration (Sun and Duan, 2007). In an anaerobic glove bag, sediment samples were homogenized, and 2.0 g sediment and 8.0 ml anoxic artificial seawater medium were added to cutoff Hungate tubes (Fig. S1B), similar to (Bowles *et al.*, 2011). The medium, modified from (Widdel and Bak, 1992), contained 2 mM HCO_3^-, 1.5 mM HS^-, and 10 mM SO_4^{2-}. Methane gas (99.7% pure) was sampled into a gastight ALTEF polypropylene bag (Restek) and transferred to glass cutoff Hungate incubation tubes (Bellco) using gastight syringes. Once fully dissolved, medium methane concentrations were 0, 1.5, or 5 mM for the different treatments. Tubes were placed upside-down in vessels, pressurized to allow methane to dissolve completely and instantaneously, and incubated at 4˚C for 30, 118, or 222 days. Incubation microcosms were conducted in triplicate. 222-day incubations were started in October 2016, while 30- and 118-day incubations began in February 2017. The cold room temperature fluctuated between 4-6˚C during storage and incubation, with a single excursion to 8˚C for several days in January 2017. During each week of incubation, pressure vessels were gently shaken to resuspend sediment slurries and repressurized to 4.0 MPa as necessary.

Medium from 118-day incubations was sampled once (at 61 days), and medium for 222-day incubations was sampled twice (at 101 and 188 days). After letting sediment settle, as much of the remaining methane gas and medium as possible was removed (4.5 to 7 ml) before replenishing with fresh methane and medium. Medium was sampled from incubation tubes with a needle and syringe and passed through a 0.2 µm filter. Samples for sulfate measurements were frozen at -20˚C in Eppendorf tubes. Medium for sulfide measurements was preserved using a saturated zinc acetate solution, centrifuged, and stored at 4˚C. Medium for dissolved inorganic carbon measurements was poisoned with a saturated mercuric chloride

solution. Sediment slurries were transferred to 15 ml falcon tubes, centrifuged, remaining supernatant poured off, and pellets frozen at -80˚C.

Geochemistry

Sediment porewater was collected using rhizon samplers spaced 10-25 cm through the sediment column (or every 1-2 cm for PC1029). Total porewater alkalinity (TA) was titrated onboard. Depending on the expected TA, we used 0.1 to 0.5 ml of porewater for titration in an open beaker with constant stirring. pH was manually recorded with every addition of 1.2 mM HCl. Seven to ten measurements were performed for every sample. TA was calculated from the recorded pH, and the amount of acid was added using the Gran function. Details of the calculation were reported previously in (Latour *et al.*, 2018). Increases in porewater alkalinity determined by onboard titrations were used to roughly constrain the SMT depths (within 30 cm) for sampling purposes. Total sulfide (ΣHS) concentrations from porewaters were measured spectrophotometrically using the method of (Cline, 1969). Samples were preserved onboard with a 23.8 mM zinc acetate solution onboard less than 30 minutes after the syringes were disconnected from rhizons, and then kept frozen until shore-based analysis. Dissolved iron (II) was determined spectrophotometrically at 595 nm onboard with a ferrospectral complex in 1% ascorbic acid. Details of sulfide and iron (II) analyses are also available in (Latour *et al.*, 2018). Porewater sulfate was analyzed with a Dionex ICS1100 ion chromatograph (IC) at the Geological Survey of Norway (NGU). An IonPac AS23 column was equipped on the IC with the eluent (4.5 mM $NaCO_3$ and 0.8 mM $NaHCO_3$) flow set to be 1 mL/min.

Sulfide from incubation medium was analyzed by the USEPA methylene blue method (Association *et al.*, 1989) using commercial reagents (Hach) and a Hach 4000 UV/Vis spectrophotometer set to 690 nm after calibration with a sulfide standard (Sigma). Sulfate from incubation medium was measured on an Integrion HPIC RFIC Ion Chromatograph (Thermo Fisher Scientific) using a Dionex IonPac AS18 Analytical Column 4X250mm column. A KOH buffer was used as an eluent, and ranged from 22 to 40 mM throughout the 20-minute run. Sulfate eluted at 10.5 min. Calibrations were prepared with five laboratory standards (Dionex), and replicate IC measurements varied on average by 0.6%. To obtain concentrations and $\delta^{13}C$ isotopic signatures, DIC samples were added to Exetainer vials (Labco), purged with helium, mixed with orthophosphoric acid to release CO_2, equilibrated for 10 h, and measured using a GasBench-DeltaV system as explained in (Torres *et al.*, 2005). $\delta^{13}C$ values are expressed in ‰ relative to PDB. Sulfate reduction, sulfide production, and DIC production rates were calculated by taking the difference of the medium concentrations of these constituents across incubation intervals and dividing by the mass of bulk sediment and time interval incubated. For each interval, the amounts of sulfate reduced and methane added were compared stoichiometrically to determine the percentage of methane that may be oxidized by sulfate. $\delta^{13}C$-CH_4 was measured using a MAT 253 isotope ratio mass spectrometer outfitted with a ConFlo IV interface (all components Thermo Fisher Scientific Inc.) at MARUM, University of Bremen, Germany and determined to be -35‰ VPDB (T. Pape, personal communication). A $\delta^{13}C$-CH_4 of -35‰ was used for all ε calculations because methane of the same isotopic signature was resupplied during incubation stages. Kinetic isotope effects (notated here as ε, epsilon) were determined by subtracting $\delta^{13}C$-CH_4 from $\delta^{13}C$-DIC measured after separate incubation intervals, and then corrected for the temperature-dependent carbon isotope fractionation between DIC and CO_2 at

4˚C (Zeebe and Wolf-Gladrow, 2001) to allow comparison with previously determined ε values (Whiticar, 1999):

$\varepsilon = (\delta^{13}C\text{-}DIC) - (\delta^{13}C\text{-}CH_4) + 7$ (Equation 2)

DNA Extraction, Amplification, Sequencing, and Analysis

DNA was extracted from sediments in a clean laminar flow hood using a Qiagen DNeasy PowerSoil kit (Hilden, Germany) following the manufacturer's protocol. The Earth Microbiome Project 16S Illumina protocol was used to prepare amplicons for sequencing. Briefly, V4 regions of bacterial and archaeal 16S rRNA genes were amplified in triplicate 25 ul reactions using universal 515-forward and 806-reverse primers (Caporaso *et al.*, 2011) modified with dual-indexed Illumina sequencing adapters (Kozich *et al.*, 2013). The thermal cycling protocol of Caporaso et al. 2011 (Caporaso *et al.*, 2011) was followed without modifications. After confirming amplification with agarose gel electrophoresis, triplicate PCR products were pooled and purified with a Qiagen QIAquick PCR purification kit. Amplicon concentrations were quantified with a Qubit fluorometer using the Qubit dsDNA high sensitivity assay kit and pooled in equimolar amounts. Illumina MiSeq V2 paired-end 250 bp sequencing was performed by technicians at Oregon State University's Center for Genome Research and Biocomputing (CGRB). A sediment-free DNA extraction blank was amplified and included in the sequencing run. Raw fastq sequences were uploaded to the NCBI Sequence Read Archive (SRA) under the BioProject number PRJNA532941.

16S gene sequences were processed with mothur (Schloss *et al.*, 2009) (v.1.39.3) following an established pipeline (Kozich *et al.*, 2013). Reads were clustered into operational taxonomic units (OTUs) at a 97% similarity level and taxonomically classified using the SILVA database (v. 128) (Quast *et al.*, 2013). We manually examined sequences known to be contaminants in DNA extraction kits and in subsurface ecosystems (Salter *et al.*, 2014; Sheik *et al.*, 2018). *Comamonas* represented the only suspicious genus, and because it was only present in an extraction blank and at low abundance, no contaminant sequences were removed from the dataset. After removal of singleton OTUs, communities were rarefied to 4,738 reads and relative abundances were calculated. Alpha diversity metrics (number of OTUs and Chao1, Shannon, and Simpson indices) were then determined. To compare beta diversity, a tree file containing the most common individual sequence from each OTU was constructed using clearcut (Evans *et al.*, 2006). Weighted Unifrac (Lozupone *et al.*, 2007) distances were calculated from the untransformed OTU table to obtain coordinates for non-metric multidimensional scaling (NMDS) ordination. ANOSIM (Clarke, 1993) was used to test for differences in community structure between incubation treatments relating to time or methane addition. Metastats (White *et al.*, 2009) was used to determine whether individual OTUs were differentially abundant between communities corresponding to these treatments.

Because microbial community composition can change appreciably during storage at these temperatures and on these timescales (Mills *et al.*, 2012), unincubated sediments were subsampled and frozen at several times during storage to determine whether changes were brought about by incubation conditions specifically (Fig. S5). OTUs belonging to genera that changed by more than 1% in abundance during sediment sample storage were omitted from results that reported changes in OTU percent abundances.

Droplet Digital PCR

Droplet digital PCR (ddPCR) was used to quantify abundances of functional genes *dsrAB* and *mcrA* using primer pairs described by Kondo et al. (Kondo *et al.*, 2004) and Luton et al. (Luton *et al.*, 2002), respectively. Reactions of 22 ul volume were prepared in a clean PCR hood in 96-well plates using 1x Bio-Rad QX200 ddPCR EvaGreen Supermix, 200 nM primers, and 0.88 ul of tenfold-diluted genomic DNA. Droplets were generated on a QX200 AutoDG Droplet Generator using automated droplet generation oil for EvaGreen Supermix (Bio-Rad). Thermal cycling was performed immediately afterwards on a Veriti 96-well thermal cycler. Protocols began with a single initialization step at 95˚C for 5 min and then proceeded to 40 cycles of denaturation at 95˚C for 30 sec, annealing for 1 min (at a temperature of 53˚C for *mcrA* and 58˚C for *dsrAB*), and for *mcrA* only, an extension at 72˚C for 75 sec. Signal stabilization steps (4˚C for 5 minutes, then 90˚C for 5 minutes) were then performed before maintaining a 4˚C hold. To ensure uniform heating of all droplets, the ramp rate for all amplification cycles was set to 2˚C/minute. Reactions were held at 4˚C overnight and read with the Bio-Rad QX200 Droplet Reader after 12 h. Droplet generation and reading were performed at OSU's CGRB core facility. Normalization was performed by inspecting fluorescence distributions using Quantasoft software (Bio-Rad). Threshold fluorescence values were manually imposed by visually inspecting distributions of DNA extraction blank and no-template-added control samples. Amplicon copy numbers per well were then converted to copies per gram bulk sediment.

607 **References**

608 Aoki, M., Ehara, M., Saito, Yumi, Yoshioka, H., Miyazaki, M., Saito, Yayoi, et al. (2014) A Long-
609 Term Cultivation of an Anaerobic Methane-Oxidizing Microbial Community from Deep-
610 Sea Methane-Seep Sediment Using a Continuous-Flow Bioreactor. *PLOS ONE* **9**:
611 e105356.
612 Association, A.P.H., Association, A.W.W., and Federation, W.P.C. (1989) Standard methods for
613 the examination of water and wastewater. 17th edition., American Public Health
614 Association.
615 Babbin, A.R., Jayakumar, A., and Ward, B.B. (2016) Organic Matter Loading Modifies the
616 Microbial Community Responsible for Nitrogen Loss in Estuarine Sediments. *Microb Ecol*
617 **71**: 555–565.
618 Berndt, C., Feseker, T., Treude, T., Krastel, S., Liebetrau, V., Niemann, H., et al. (2014) Temporal
619 Constraints on Hydrate-Controlled Methane Seepage off Svalbard. *Science* **343**: 284–
620 287.
621 Bhattarai, S., Cassarini, C., Rene, E.R., Kümmel, S., Esposito, G., and Lens, P.N.L. (2018)
622 Enrichment of ANME-2 dominated anaerobic methanotrophy from cold seep sediment
623 in an external ultrafiltration membrane bioreactor. *Engineering in Life Sciences* **18**: 368–
624 378.
625 Bhattarai, S., Cassarini, C., Rene, E.R., Zhang, Y., Esposito, G., and Lens, P.N.L. (2018) Enrichment
626 of sulfate reducing anaerobic methane oxidizing community dominated by ANME-1
627 from Ginsburg Mud Volcano (Gulf of Cadiz) sediment in a biotrickling filter. *Bioresource*
628 *Technology*.
629 Bhattarai, S., Zhang, Y., and Lens, P.N.L. (2018) Effect of pressure and temperature on anaerobic
630 methanotrophic activities of a highly enriched ANME-2a community. *Environ Sci Pollut*
631 *Res* **25**: 30031–30043.
632 Boetius, A. and Wenzhöfer, F. (2013) Seafloor oxygen consumption fuelled by methane from
633 cold seeps. *Nature Geoscience* **6**: 725–734.
634 Borowski, W.S., Paull, C.K., and Ussler, W. (1997) Carbon cycling within the upper methanogenic
635 zone of continental rise sediments; An example from the methane-rich sediments
636 overlying the Blake Ridge gas hydrate deposits. *Marine Chemistry* **57**: 299–311.
637 Borowski, W.S., Paull, C.K., and Ussler, W. (1996) Marine pore-water sulfate profiles indicate in
638 situ methane flux from underlying gas hydrate. *Geology* **24**: 655–658.
639 Bowles, M.W., Samarkin, V.A., and Joye, S.B. (2011) Improved measurement of microbial
640 activity in deep-sea sediments at in situ pressure and methane concentration:
641 Measuring activity in deep-sea sediments. *Limnology and Oceanography: Methods* **9**:
642 499–506.
643 Caporaso, J.G., Lauber, C.L., Walters, W.A., Berg-Lyons, D., Lozupone, C.A., Turnbaugh, P.J., et
644 al. (2011) Global patterns of 16S rRNA diversity at a depth of millions of sequences per
645 sample. *Proceedings of the National Academy of Sciences* **108**: 4516–4522.
646 Case, D.H., Ijiri, A., Morono, Y., Tavormina, P., Orphan, V.J., and Inagaki, F. (2017) Aerobic and
647 Anaerobic Methanotrophic Communities Associated with Methane Hydrates Exposed on
648 the Seafloor: A High-Pressure Sampling and Stable Isotope-Incubation Experiment. *Front*
649 *Microbiol* **8**:.

650 Clarke, K.R. (1993) Non-parametric multivariate analyses of changes in community structure.
651 *Australian Journal of Ecology* **18**: 117–143.
652 Cline, J.D. (1969) Spectrophotometric Determination of Hydrogen Sulfide in Natural Waters1.
653 *Limnology and Oceanography* **14**: 454–458.
654 Dale, A.W., Van Cappellen, P., Aguilera, D.R., and Regnier, P. (2008) Methane efflux from
655 marine sediments in passive and active margins: Estimations from bioenergetic
656 reaction–transport simulations. *Earth and Planetary Science Letters* **265**: 329–344.
657 Deusner, C., Meyer, V., and Ferdelman, T.G. (2010) High-pressure systems for gas-phase free
658 continuous incubation of enriched marine microbial communities performing anaerobic
659 oxidation of methane. *Biotechnol Bioeng* **105**: 524–533.
660 Du, Z.-J., Wang, Y., Dunlap, C., Rooney, A.P., and Chen, G.-J. (2014) Draconibacterium orientale
661 gen. nov., sp. nov., isolated from two distinct marine environments, and proposal of
662 Draconibacteriaceae fam. nov. *INTERNATIONAL JOURNAL OF SYSTEMATIC AND*
663 *EVOLUTIONARY MICROBIOLOGY* **64**: 1690–1696.
664 Evans, J., Sheneman, L., and Foster, J. (2006) Relaxed Neighbor Joining: A Fast Distance-Based
665 Phylogenetic Tree Construction Method. *J Mol Evol* **62**: 785–792.
666 Evans, P.N., Parks, D.H., Chadwick, G.L., Robbins, S.J., Orphan, V.J., Golding, S.D., and Tyson,
667 G.W. (2015) Methane metabolism in the archaeal phylum Bathyarchaeota revealed by
668 genome-centric metagenomics. *Science* **350**: 434–438.
669 Fuchs, A., Lyautey, E., Montuelle, B., and Casper, P. (2016) Effects of increasing temperatures
670 on methane concentrations and methanogenesis during experimental incubation of
671 sediments from oligotrophic and mesotrophic lakes. *J Geophys Res Biogeosci* **121**:
672 2016JG003328.
673 Girguis, P.R., Cozen, A.E., and DeLong, E.F. (2005) Growth and Population Dynamics of
674 Anaerobic Methane-Oxidizing Archaea and Sulfate-Reducing Bacteria in a Continuous-
675 Flow Bioreactor. *Appl Environ Microbiol* **71**: 3725–3733.
676 Girguis, P.R., Orphan, V.J., Hallam, S.J., and DeLong, E.F. (2003) Growth and Methane Oxidation
677 Rates of Anaerobic Methanotrophic Archaea in a Continuous-Flow Bioreactor. *Appl*
678 *Environ Microbiol* **69**: 5472–5482.
679 Hallam, S.J., Girguis, P.R., Preston, C.M., Richardson, P.M., and DeLong, E.F. (2003) Identification
680 of Methyl Coenzyme M Reductase A (mcrA) Genes Associated with Methane-Oxidizing
681 Archaea. *Appl Environ Microbiol* **69**: 5483–5491.
682 Hammes, F., Vital, M., and Egli, T. (2010) Critical Evaluation of the Volumetric "Bottle Effect" on
683 Microbial Batch Growth. *Appl Environ Microbiol* **76**: 1278–1281.
684 Haroon, M.F., Hu, S., Shi, Y., Imelfort, M., Keller, J., Hugenholtz, P., et al. (2013) Anaerobic
685 oxidation of methane coupled to nitrate reduction in a novel archaeal lineage. *Nature*
686 **500**: 567–570.
687 Harrison, B.K., Zhang, H., Berelson, W., and Orphan, V.J. (2009) Variations in Archaeal and
688 Bacterial Diversity Associated with the Sulfate-Methane Transition Zone in Continental
689 Margin Sediments (Santa Barbara Basin, California). *Applied and Environmental*
690 *Microbiology* **75**: 1487–1499.
691 Heitmann, T. and Blodau, C. (2006) Oxidation and incorporation of hydrogen sulfide by
692 dissolved organic matter. *Chemical Geology* **235**: 12–20.

693 Hensen, C., Zabel, M., Pfeifer, K., Schwenk, T., Kasten, S., Riedinger, N., et al. (2003) Control of
694 sulfate pore-water profiles by sedimentary events and the significance of anaerobic
695 oxidation of methane for the burial of sulfur in marine sediments. *Geochimica et*
696 *Cosmochimica Acta* **67**: 2631–2647.
697 Holmes, D.E., Nicoll, J.S., Bond, D.R., and Lovley, D.R. (2004) Potential Role of a Novel
698 Psychrotolerant Member of the Family Geobacteraceae, Geopsychrobacter
699 electrodiphilus gen. nov., sp. nov., in Electricity Production by a Marine Sediment Fuel
700 Cell. *Appl Environ Microbiol* **70**: 6023–6030.
701 Hong, W.-L., Sauer, S., Panieri, G., Ambrose, W.G., James, R.H., Plaza-Faverola, A., and
702 Schneider, A. (2016) Removal of methane through hydrological, microbial, and
703 geochemical processes in the shallow sediments of pockmarks along eastern Vestnesa
704 Ridge (Svalbard). *Limnol Oceanogr* n/a-n/a.
705 Hong, W.-L., Torres, M.E., Carroll, J., Crémière, A., Panieri, G., Yao, H., and Serov, P. (2017)
706 Seepage from an arctic shallow marine gas hydrate reservoir is insensitive to
707 momentary ocean warming. *Nat Commun* **8**: 15745.
708 Hong, W.-L., Torres, M.E., Portnov, A., Waage, M., Haley, B., and Lepland, A. (2018) Variations in
709 Gas and Water Pulses at an Arctic Seep: Fluid Sources and Methane Transport.
710 *Geophysical Research Letters* **45**: 4153–4162.
711 Hunter, S.J., Goldobin, D.S., Haywood, A.M., Ridgwell, A., and Rees, J.G. (2013) Sensitivity of the
712 global submarine hydrate inventory to scenarios of future climate change. *Earth and*
713 *Planetary Science Letters*.
714 Isaksen, M.F. and Teske, A. (1996) Desulforhopalus vacuolatus gen. nov., sp. nov., a new
715 moderately psychrophilic sulfate-reducing bacterium with gas vacuoles isolated from a
716 temperate estuary. *Arch Microbiol* **166**: 160–168.
717 James, R.H., Bousquet, P., Bussmann, I., Haeckel, M., Kipfer, R., Leifer, I., et al. (2016) Effects of
718 climate change on methane emissions from seafloor sediments in the Arctic Ocean: A
719 review. *Limnol Oceanogr* **61**: S283–S299.
720 Klasek, S.A., Torres, M.E., Loher, M., Bohrmann, G., Pape, T., and Colwell, F.S. (2019) Deep-
721 sourced fluids from a convergent margin host distinct subseafloor microbial
722 communities that change upon mud flow expulsion. *Front Microbiol* **10**:.
723 Knief, C., Kolb, S., Bodelier, P.L.E., Lipski, A., and Dunfield, P.F. (2006) The active
724 methanotrophic community in hydromorphic soils changes in response to changing
725 methane concentration. *Environmental Microbiology* **8**: 321–333.
726 Knittel, K. and Boetius, A. (2009) Anaerobic Oxidation of Methane: Progress with an Unknown
727 Process. *Annual Review of Microbiology* **63**: 311–334.
728 Kondo, R., Nedwell, D.B., Purdy, K.J., and Silva, S.Q. (2004) Detection and Enumeration of
729 Sulphate-Reducing Bacteria in Estuarine Sediments by Competitive PCR.
730 *Geomicrobiology Journal* **21**: 145–157.
731 Kozich, J.J., Westcott, S.L., Baxter, N.T., Highlander, S.K., and Schloss, P.D. (2013) Development
732 of a Dual-Index Sequencing Strategy and Curation Pipeline for Analyzing Amplicon
733 Sequence Data on the MiSeq Illumina Sequencing Platform. *Appl Environ Microbiol* **79**:
734 5112–5120.

Krüger, M., Wolters, H., Gehre, M., Joye, S.B., and Richnow, H.-H. (2008) Tracing the slow growth of anaerobic methane-oxidizing communities by 15N-labelling techniques. *FEMS Microbiology Ecology* **63**: 401–411.

Latour, P., Hong, W.-L., Sauer, S., Sen, A., Gilhooly III, W.P., Lepland, A., and Fouskas, F. (2018) Dynamic interactions between iron and sulfur cycles from Arctic methane seeps. *Biogeosciences Discussions* 1–48.

Lazar, C.S., John Parkes, R., Cragg, B.A., L'Haridon, S., and Toffin, L. (2012) Methanogenic activity and diversity in the centre of the Amsterdam Mud Volcano, Eastern Mediterranean Sea. *FEMS Microbiol Ecol* **81**: 243–254.

Leloup, J., Quillet, L., Oger, C., Boust, D., and Petit, F. (2004) Molecular quantification of sulfate-reducing microorganisms (carrying dsrAB genes) by competitive PCR in estuarine sediments. *FEMS Microbiol Ecol* **47**: 207–214.

Li, X., Song, L., Wang, G., Ren, L., Yu, D., Chen, G., et al. (2016) Complete genome sequence of a deeply branched marine Bacteroidia bacterium Draconibacterium orientale type strain FH5T. *Marine Genomics* **26**: 13–16.

Lie, T.J., Clawson, M.L., Godchaux, W., and Leadbetter, E.R. (1999) Sulfidogenesis from 2-Aminoethanesulfonate (Taurine) Fermentation by a Morphologically Unusual Sulfate-Reducing Bacterium, Desulforhopalus singaporensis sp. nov. *APPL ENVIRON MICROBIOL* **65**: 7.

Lozupone, C.A., Hamady, M., Kelley, S.T., and Knight, R. (2007) Quantitative and Qualitative β Diversity Measures Lead to Different Insights into Factors That Structure Microbial Communities. *Appl Environ Microbiol* **73**: 1576–1585.

Luton, P.E., Wayne, J.M., Sharp, R.J., and Riley, P.W. (2002) The mcrA gene as an alternative to 16S rRNA in the phylogenetic analysis of methanogen populations in landfillb. *Microbiology* **148**: 3521–3530.

Maillacheruvu, K.Y. and Parkin, G.F. (1996) Kinetics of growth, substrate utilization and sulfide toxicity for propionate, acetate, and hydrogen utilizers in anaerobic systems. *Water Environment Research* **68**: 1099–1106.

Mau, S., Römer, M., Torres, M.E., Bussmann, I., Pape, T., Damm, E., et al. (2017) Widespread methane seepage along the continental margin off Svalbard - from Bjørnøya to Kongsfjorden. *Sci Rep* **7**:.

McCalley, C.K., Woodcroft, B.J., Hodgkins, S.B., Wehr, R.A., Kim, E.-H., Mondav, R., et al. (2014) Methane dynamics regulated by microbial community response to permafrost thaw. *Nature* **514**: 478–481.

Meulepas, R.J.W., Jagersma, C.G., Gieteling, J., Buisman, C.J.N., Stams, A.J.M., and Lens, P.N.L. (2009) Enrichment of anaerobic methanotrophs in sulfate-reducing membrane bioreactors. *Biotechnol Bioeng* **104**: 458–470.

Mills, H.J., Reese, B.K., and Peter, C.St. (2012) Characterization of Microbial Population Shifts during Sample Storage. *Frontiers in Microbiology* **3**:.

Müller, A.L., Kjeldsen, K.U., Rattei, T., Pester, M., and Loy, A. (2015) Phylogenetic and environmental diversity of DsrAB-type dissimilatory (bi)sulfite reductases. *ISME J* **9**: 1152–1165.

Nauhaus, K., Albrecht, M., Elvert, M., Boetius, A., and Widdel, F. (2007) In vitro cell growth of marine archaeal-bacterial consortia during anaerobic oxidation of methane with sulfate. *Environmental Microbiology* **9**: 187–196.

Nauhaus, K., Boetius, A., Krüger, M., and Widdel, F. (2002) In vitro demonstration of anaerobic oxidation of methane coupled to sulphate reduction in sediment from a marine gas hydrate area. *Environmental Microbiology* **4**: 296–305.

Nauhaus, K., Treude, T., Boetius, A., and Kruger, M. (2005) Environmental regulation of the anaerobic oxidation of methane: a comparison of ANME-I and ANME-II communities. *Environmental Microbiology* **7**: 98–106.

Nunoura, T., Oida, H., Miyazaki, J., Miyashita, A., Imachi, H., and Takai, K. (2008) Quantification of mcrA by fluorescent PCR in methanogenic and methanotrophic microbial communities. *FEMS Microbiology Ecology* **64**: 240–247.

Pernthaler, J. and Amann, R. (2005) Fate of Heterotrophic Microbes in Pelagic Habitats: Focus on Populations. *Microbiol Mol Biol Rev* **69**: 440–461.

Pfennig, N. and Biebl, H. (1976) Desulfuromonas acetoxidans gen. nov. and sp. nov., a new anaerobic, sulfur-reducing, acetate-oxidizing bacterium. *Archives of Microbiology* **110**: 3–12.

Quast, C., Pruesse, E., Yilmaz, P., Gerken, J., Schweer, T., Yarza, P., et al. (2013) The SILVA ribosomal RNA gene database project: improved data processing and web-based tools. *Nucleic Acids Res* **41**: D590–D596.

Reeburgh, W.S. (2007) Oceanic Methane Biogeochemistry. *Chem Rev* **107**: 486–513.

Roden, E.E. and Lovley, D.R. (1993) Dissimilatory Fe(III) Reduction by the Marine Microorganism Desulfuromonas acetoxidans. *Appl Environ Microbiol* **59**: 734–742.

Ruff, S.E., Biddle, J.F., Teske, A.P., Knittel, K., Boetius, A., and Ramette, A. (2015) Global dispersion and local diversification of the methane seep microbiome. *PNAS* **112**: 4015–4020.

Ruff, S.E., Felden, J., Gruber-Vodicka, H.R., Marcon, Y., Knittel, K., Ramette, A., and Boetius, A. (2018) In situ development of a methanotrophic microbiome in deep-sea sediments. *The ISME Journal* 1.

Salter, S.J., Cox, M.J., Turek, E.M., Calus, S.T., Cookson, W.O., Moffatt, M.F., et al. (2014) Reagent and laboratory contamination can critically impact sequence-based microbiome analyses. *BMC Biology* **12**: 87.

Schloss, P.D., Westcott, S.L., Ryabin, T., Hall, J.R., Hartmann, M., Hollister, E.B., et al. (2009) Introducing mothur: Open-Source, Platform-Independent, Community-Supported Software for Describing and Comparing Microbial Communities. *Appl Environ Microbiol* **75**: 7537–7541.

Seifert, R., Nauhaus, K., Blumenberg, M., Krüger, M., and Michaelis, W. (2006) Methane dynamics in a microbial community of the Black Sea traced by stable carbon isotopes in vitro. *Organic Geochemistry* **37**: 1411–1419.

Serov, P., Vadakkepuliyambatta, S., Mienert, J., Patton, H., Portnov, A., Silyakova, A., et al. (2017) Postglacial response of Arctic Ocean gas hydrates to climatic amelioration. *PNAS* **114**: 6215–6220.

819 Shakhova, N., Semiletov, I., Salyuk, A., Yusupov, V., Kosmach, D., and Gustafsson, Ö. (2010)
820 Extensive Methane Venting to the Atmosphere from Sediments of the East Siberian
821 Arctic Shelf. *Science* **327**: 1246–1250.
822 Sheik, C.S., Reese, B.K., Twing, K.I., Sylvan, J.B., Grim, S.L., Schrenk, M.O., et al. (2018)
823 Identification and Removal of Contaminant Sequences From Ribosomal Gene Databases:
824 Lessons From the Census of Deep Life. *Front Microbiol* **9**:.
825 Starnawski, P., Bataillon, T., Ettema, T.J.G., Jochum, L.M., Schreiber, L., Chen, X., et al. (2017)
826 Microbial community assembly and evolution in subseafloor sediment. *PNAS*
827 201614190.
828 Stegen, J.C., Fredrickson, J.K., Wilkins, M.J., Konopka, A.E., Nelson, W.C., Arntzen, E.V., et al.
829 (2016) Groundwater–surface water mixing shifts ecological assembly processes and
830 stimulates organic carbon turnover. *Nature Communications* **7**: 11237.
831 Stewart, F.J., Dalsgaard, T., Young, C.R., Thamdrup, B., Revsbech, N.P., Ulloa, O., et al. (2012)
832 Experimental Incubations Elicit Profound Changes in Community Transcription in OMZ
833 Bacterioplankton. *PLoS ONE* **7**: e37118.
834 Sun, R. and Duan, Z. (2007) An accurate model to predict the thermodynamic stability of
835 methane hydrate and methane solubility in marine environments. *Chemical Geology*
836 **244**: 248–262.
837 Timmers, P.H.A., Gieteling, J., Widjaja-Greefkes, H.C.A., Plugge, C.M., Stams, A.J.M., Lens, P.N.L.,
838 and Meulepas, R.J.W. (2015) Growth of Anaerobic Methane-Oxidizing Archaea and
839 Sulfate-Reducing Bacteria in a High-Pressure Membrane Capsule Bioreactor. *Appl*
840 *Environ Microbiol* **81**: 1286–1296.
841 Torres, M.E., Mix, A.C., and Rugh, W.D. (2005) Precise δ13C analysis of dissolved inorganic
842 carbon in natural waters using automated headspace sampling and continuous-flow
843 mass spectrometry. *Limnology and Oceanography: Methods* **3**: 349–360.
844 Valentine, D.L. (2002) Biogeochemistry and microbial ecology of methane oxidation in anoxic
845 environments: a review. *Antonie Van Leeuwenhoek* **81**: 271–282.
846 Vandieken, V. (2006) Desulfuromonas svalbardensis sp. nov. and Desulfuromusa ferrireducens
847 sp. nov., psychrophilic, Fe(III)-reducing bacteria isolated from Arctic sediments,
848 Svalbard. *INTERNATIONAL JOURNAL OF SYSTEMATIC AND EVOLUTIONARY*
849 *MICROBIOLOGY* **56**: 1133–1139.
850 Vanwonterghem, I., Evans, P.N., Parks, D.H., Jensen, P.D., Woodcroft, B.J., Hugenholtz, P., and
851 Tyson, G.W. (2016) Methylotrophic methanogenesis discovered in the archaeal phylum
852 Verstraetearchaeota. *Nature Microbiology* **1**: 16170.
853 Wallmann, K., Riedel, M., Hong, W.L., Patton, H., Hubbard, A., Pape, T., et al. (2018) Gas hydrate
854 dissociation off Svalbard induced by isostatic rebound rather than global warming.
855 *Nature Communications* **9**: 83.
856 Wang, F.-P., Zhang, Y., Chen, Y., He, Y., Qi, J., Hinrichs, K.-U., et al. (2014) Methanotrophic
857 archaea possessing diverging methane-oxidizing and electron-transporting pathways.
858 *ISME J* **8**: 1069–1078.
859 Wegener, G., Krukenberg, V., Ruff, S.E., Kellermann, M.Y., and Knittel, K. (2016) Metabolic
860 Capabilities of Microorganisms Involved in and Associated with the Anaerobic Oxidation
861 of Methane. *Front Microbiol* **7**:.

Westbrook, G.K., Thatcher, K.E., Rohling, E.J., Piotrowski, A.M., Pälike, H., Osborne, A.H., et al. (2009) Escape of methane gas from the seabed along the West Spitsbergen continental margin: ARCTIC METHANE GAS PLUMES. *Geophysical Research Letters* **36**: n/a-n/a.

White, J.R., Nagarajan, N., and Pop, M. (2009) Statistical Methods for Detecting Differentially Abundant Features in Clinical Metagenomic Samples. *PLoS Comput Biol* **5**:.

Whiticar, M.J. (1999) Carbon and hydrogen isotope systematics of bacterial formation and oxidation of methane. *Chemical Geology* **161**: 291–314.

Widdel, F. and Bak, F. (1992) Gram-Negative Mesophilic Sulfate-Reducing Bacteria. In, Balows,A., Trüper,H.G., Dworkin,M., Harder,W., and Schleifer,K.-H. (eds), *The Prokaryotes*. Springer New York, pp. 3352–3378.

Yoshinaga, M.Y., Holler, T., Goldhammer, T., Wegener, G., Pohlman, J.W., Brunner, B., et al. (2014) Carbon isotope equilibration during sulphate-limited anaerobic oxidation of methane. *Nature Geoscience* **7**: 190–194.

Zeebe, R.E. and Wolf-Gladrow, D. (2001) CO2 in Seawater: Equilibrium, Kinetics, Isotopes, Gulf Professional Publishing.

Zhang, Y., Henriet, J.-P., Bursens, J., and Boon, N. (2010) Stimulation of in vitro anaerobic oxidation of methane rate in a continuous high-pressure bioreactor. *Bioresource Technology* **101**: 3132–3138.

Zhang, Y., Maignien, L., Stadnitskaia, A., Boeckx, P., Xiao, X., and Boon, N. (2014) Stratified Community Responses to Methane and Sulfate Supplies in Mud Volcano Deposits: Insights from an In Vitro Experiment. *PLoS ONE* **9**: e113004.

Table 1. Summary of key geochemical and microbiological measurements across all incubated sediment types that changed significantly based on added methane concentration [CH_4], incubation time, or both. ND: not detected. Because all methane-dependent changes observed were also time-dependent, methane concentration alone is not listed as a variable.

	SR and solute concs.	ε	Microbial community	*mcrA*	*dsrAB*	ANME % abundance
	[CH_4] & time	*[CH_4] & time*	*time*	*[CH_4] & time*	*time*	*[CH_4] & time*
IA	ND	ND	Shifts the most	ND	↑	ND
A	↓ in SO_4^{2-} ↑ in HS^-	↓	Shifts slightly	ND	ND	↑
PA	ND	ND	Shifts significantly	↑	↑	ND
	Figs. 2, S2-4	*Fig. 3*	*Fig. 5*	*Fig. 7A*	*Fig. S6*	*Fig. 7B*

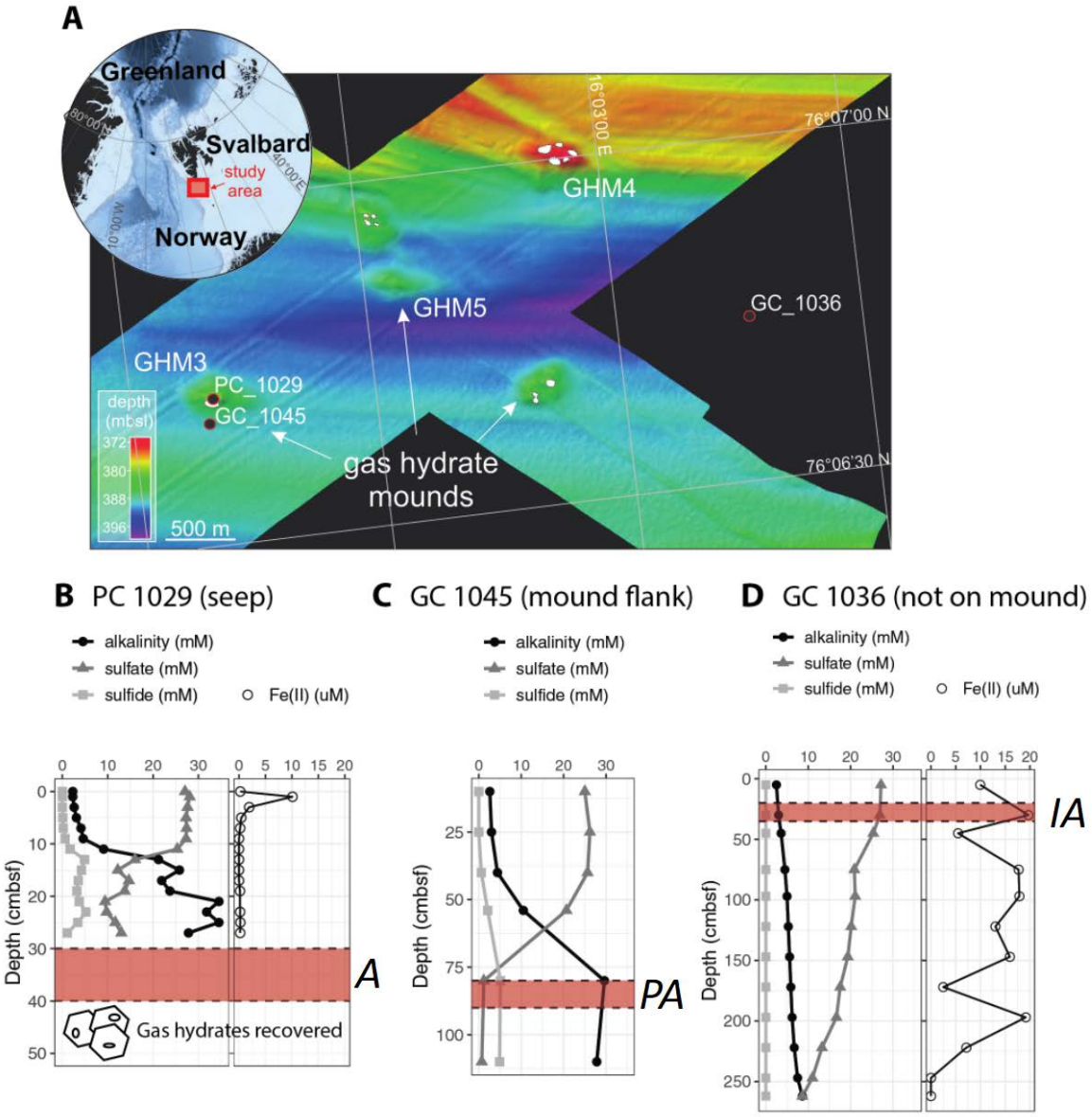

Figure 1. Map of the Storfjordrenna trough mouth fan, south of Svalbard, showing locations of the three cores taken with white polygons indicating areas of methane seepage observed during sampling (A). Sulfate, sulfide, alkalinity, and iron (II) porewater profiles are shown successively in (B-D): PC1029, a push core from a seep at GHM 3; GC1045, a gravity core from the flank of the same GHM, and GC1036, a reference core near the mounds. Red bands within dotted lines indicate sediment sample depths collected for incubations. Sediment sample names correspond to inferred methanotrophic capacity: active (*A*), previously active (*PA*), and inactive (*IA*).

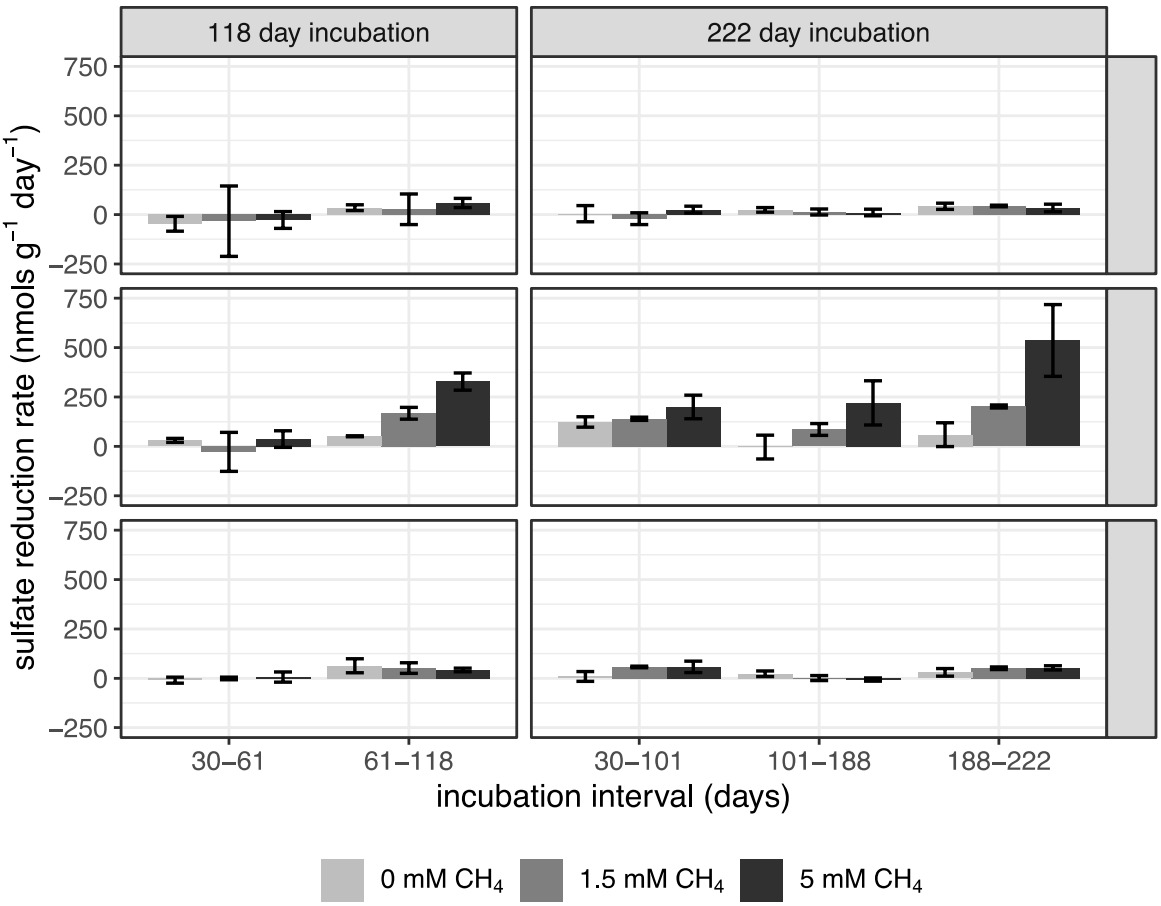

Figure 2. Sulfate reduction rates measured across incubation intervals. Panels are separated horizontally by total incubation time (118 or 222 days) and vertically by sediment type. Gray shades designate added methane concentrations, and error bars represent 95% confidence intervals from triplicate measurements. Methane-dependent SR was only observed in the *A* sediments collected from an area of active seepage.

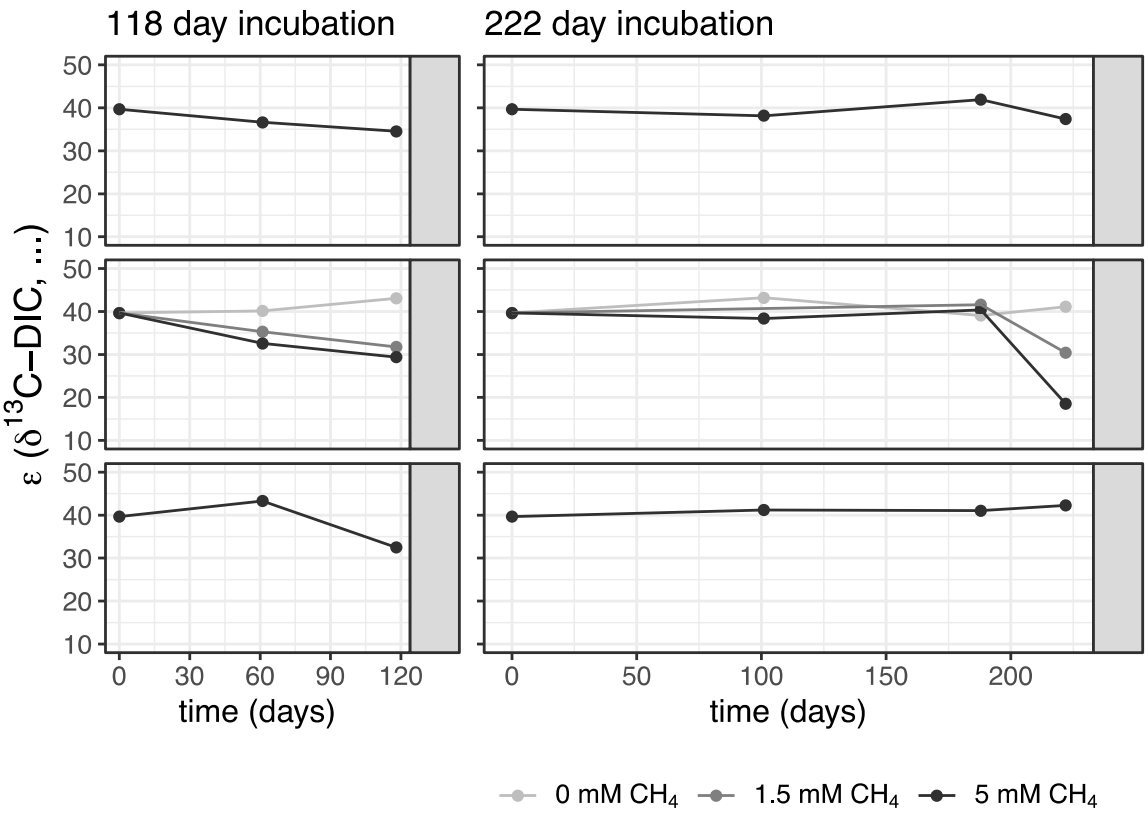

Figure 3. Changes in ε, the kinetic isotope fractionation during anaerobic oxidation of methane to DIC, over incubation time. Panels are separated horizontally by total incubation lengths (118 or 222 days) and vertically by sediment type, and gray shades designate methane concentrations. Decreasing values of ε during incubations of *A* sediment samples indicate a more prominent influence from AOM.

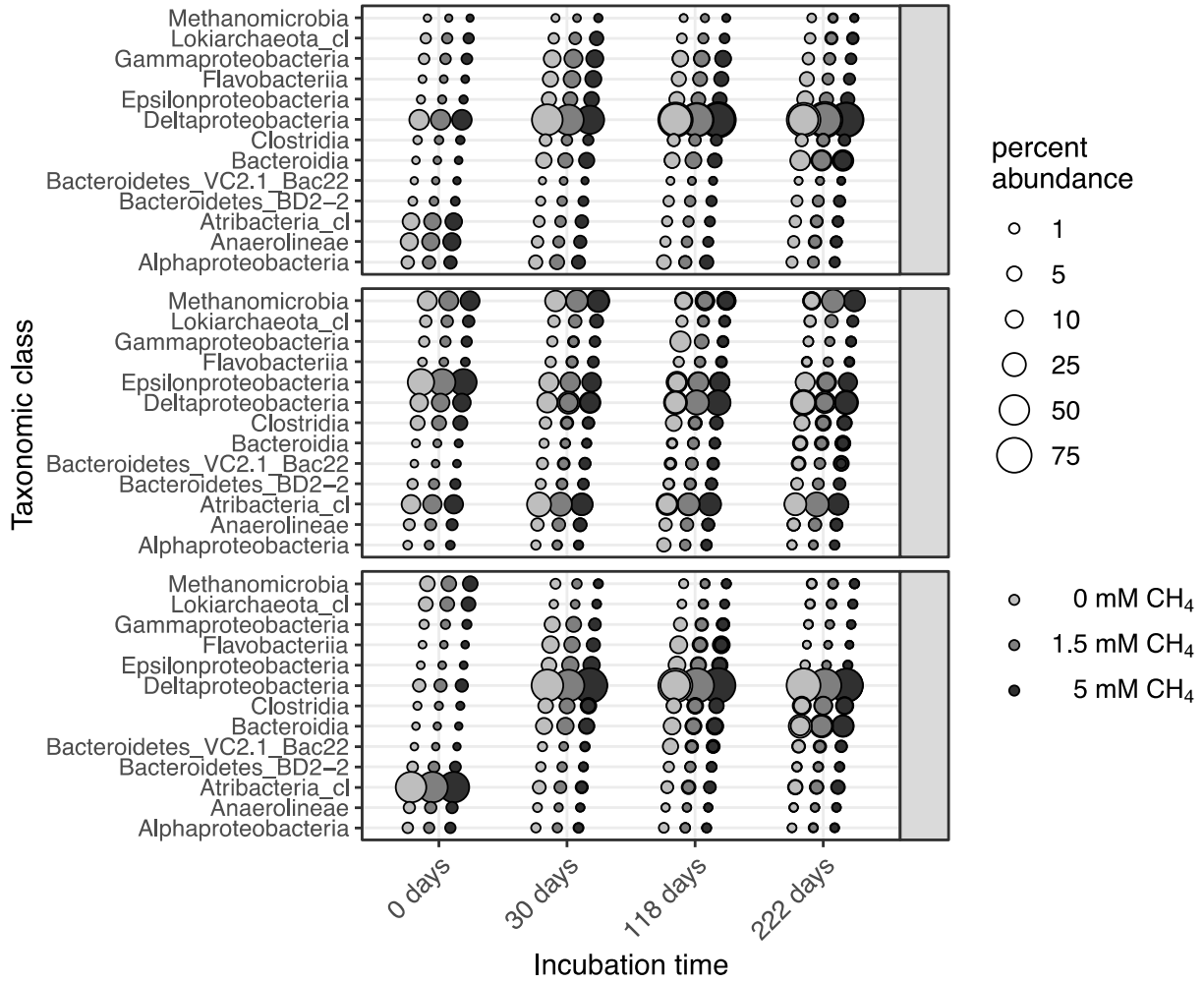

Figure 4. Percent abundances of class-level taxonomic divisions across all sediment types, times incubated, and initial methane concentrations. These sequences constitute >90% of the dataset. The extent of variation between duplicate or triplicate microbial communities incubated under the same conditions is conveyed by widths of black outlines.

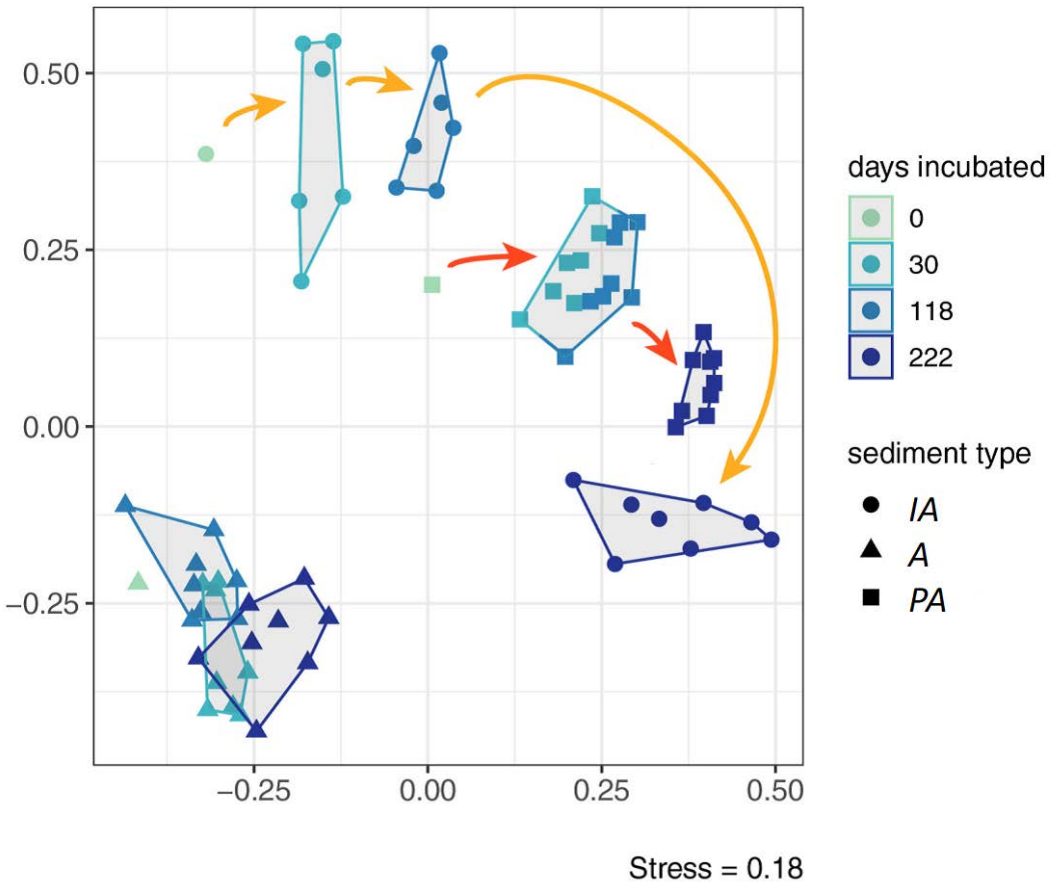

Figure 5. NMDS ordination of weighted Unifrac distances between communities. Symbols are colored according to incubation length, and shaped according to sediment type. Polygons indicate statistically distinct community structures as determined by ANOSIM using α=0.05 with a Bonferroni correction for multiple comparisons (Table S1). Initial methane concentrations are not indicated because methane did not structure community composition across any sediment type (Table S1).

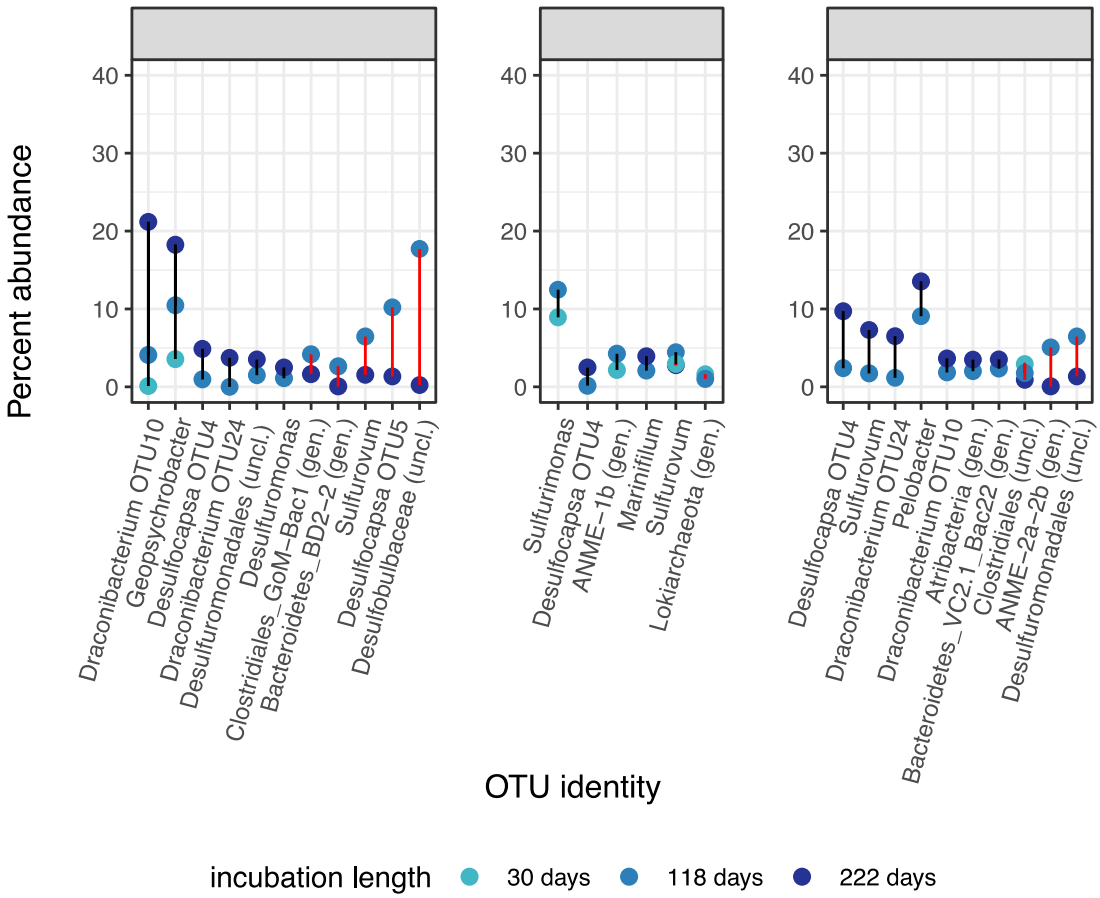

924
925 Figure 6. Percent abundance and taxonomic identity of the most common OTUs (each >1% of
926 their communities) whose abundances changed significantly (α=0.05) when incubated for
927 different lengths of time. Blue dots represent incubations of different lengths, and are
928 connected by black or red vertical lines that respectively show increases or decreases in OTU
929 percent abundance over the corresponding interval. Where multiple OTUs share taxonomic
930 identity, OTU numbers are included. Added methane concentrations are omitted from this
931 figure, as they changed relative abundances of only three other OTUs (discussed earlier in text).

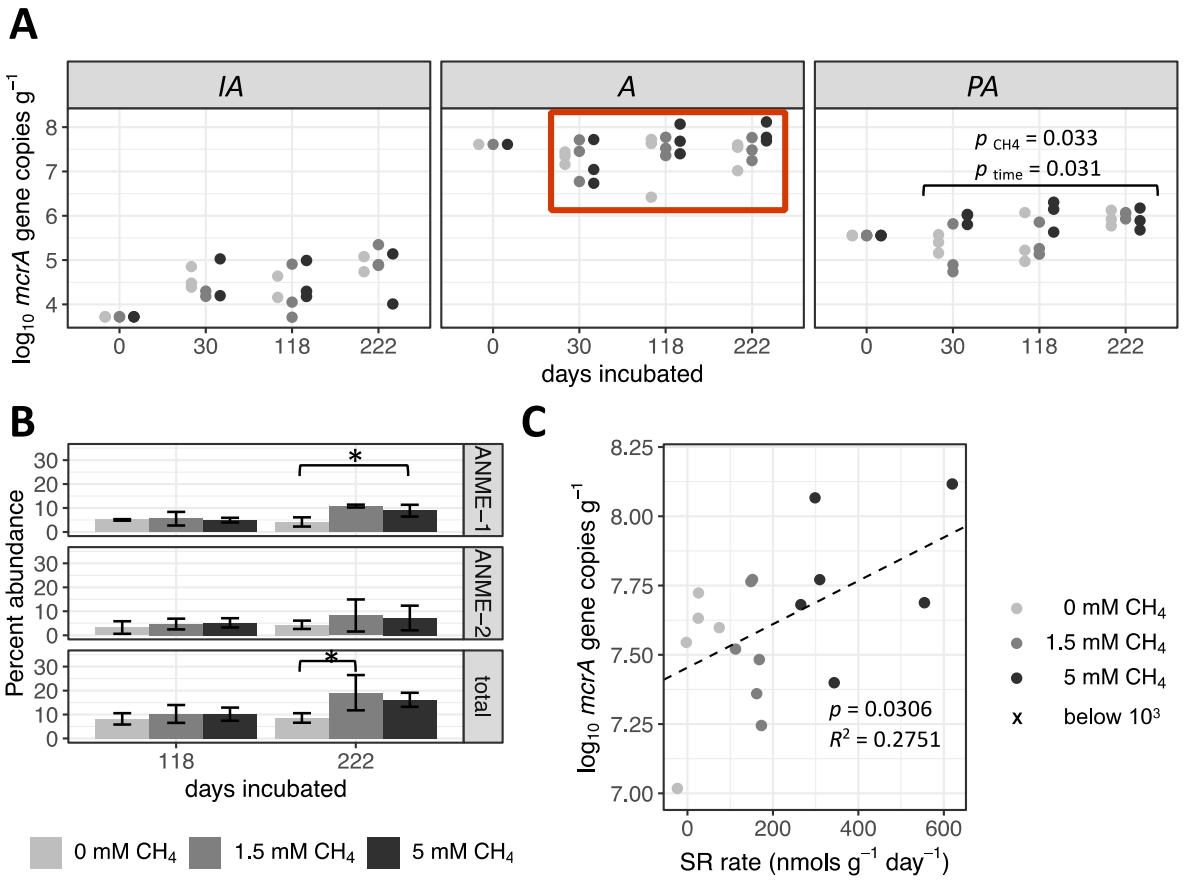

Figure 7. Log-normalized abundances of *mcrA* genes (g^{-1} bulk sediment) in incubated samples, enumerated by ddPCR (A). Points are shaded by initial methane concentrations, and X denotes readings below detection (10^3 genes g^{-1}). One measurement was taken for preincubated (day 0) samples. Significant differences in gene abundances across incubation times and methane concentrations, excluding day 0 samples, are shown as brackets with corresponding p-values (two-way factorial ANOVA, α=0.05). Table S2 gives additional information on these tests. Orange box shows a subset of active (*A*) sediments incubated for 118 or 222 days. Of this subset, Panel (B) shows changes in percent abundances of ANME clades, with 95% confidence intervals shown for three replicates and brackets with asterisks denoting statistical significance among close comparisons. (C) relates sulfate reduction rates and *mcrA* gene abundances of the same subset through a linear regression.

Acknowledgements

We express gratitude to the officers and crew of R/V Helmer Hanssen on the CAGE cruise 16-5, cruise leader Michael Carroll, chief engineers Bjørn Runar Olsen, Pedro De La Torre, Frode Volden, and researcher Stein Nornæs from the Centre for Autonomous Marine Operations and Systems (AMOS) for helping with sample acquisition and ROV operation. We also thank Stefan Bünz for providing bathymetric data, and Alexey Portnov for mapping the study area. Benjamin Russell at the Oregon State University (OSU) College of Earth, Ocean, and Atmospheric Science (CEOAS) Machine and Technical Development Facility designed parts for the Benthos pressure vessel. We also thank Mark Dasenko, Anne-Marie Girard Pohjanpelto, and Jessica Nixon at the OSU Center for Genome Resources and Biocomputing (CGRB) for support with DNA sequencing and droplet digital PCR. Andy Ross ran carbon isotope measurements at the OSU stable isotope laboratory, and Thomas Pape aided with methane isotope measurements. Iria Giménez provided instruction in measuring sulfate. Logan Peoples (Scripps Institute of Oceanography) provided assistance with incubation setup, and Yasaman Jaladat (UCSD) provided additional help with sample storage. This work is supported by the Research Council of Norway (RCN) through its Centres of Excellence funding scheme project no. 223259, and also by the U.S. Department of Energy (DE-FE0013531) and the Deep Carbon Observatory's Deep Life Cultivation Internship (supported through the Sloan Foundation).